Comparative analysis defines a broader FMRFamide-gated sodium channel family and determinants of neuropeptide sensitivity

Received for publication, March 26, 2022, and in revised form, May 19, 2022 Published, Papers in Press, May 27, 2022,
https://doi.org/10.1016/j.jbc.2022.102086

Mowgli Dandamudi[1], **Harald Hausen**[1,2], **and Timothy Lynagh**[1,*]

From the [1]*Sars International Centre for Marine Molecular Biology, and* [2]*Department of Earth Science, University of Bergen, Bergen, Norway*

Edited by Elizabeth Coulson

FMRFamide (Phe-Met-Arg-Phe-amide, FMRFa) and similar neuropeptides are important physiological modulators in most invertebrates, but the molecular basis of FMRFa activity at its receptors is unknown. We therefore sought to identify the molecular determinants of FMRFa potency against one of its native targets, the excitatory FMRFa-gated sodium channel (FaNaC) from gastropod mollusks. Using molecular phylogenetics and electrophysiological measurement of neuropeptide activity, we identified a broad FaNaC family that includes mollusk and annelid channels gated by FMRFa, FVRIamides, and/or Wamides (or myoinhibitory peptides). A comparative analysis of this broader FaNaC family and other channels from the overarching degenerin (DEG)/epithelial sodium channel (ENaC) superfamily, incorporating mutagenesis and experimental dissection of channel function, identified a pocket of amino acid residues that determines activation of FaNaCs by neuropeptides. Although this pocket has diverged in distantly related DEG/ENaC channels that are activated by other ligands but enhanced by FMRFa, such as mammalian acid-sensing ion channels, we show that it nonetheless contains residues that determine enhancement of those channels by similar peptides. This study thus identifies amino acid residues that determine FMRFa neuropeptide activity at FaNaC receptor channels and illuminates the evolution of ligand recognition in one branch of the DEG/ENaC superfamily of ion channels.

Neuropeptides are a large, diverse group of intercellular signaling molecules found in most animals (1). They commonly range in length from 4 to 40 aa residues and are generally the cleavage product of a long propeptide containing multiple shorter peptides between peptidase cleavage sites. By diffusing to and binding their receptor targets on other cells, which are most often G-protein coupled receptors, neuropeptides modulate numerous physiological functions. These include neuronal excitability, ciliary beating and locomotion, and muscle contraction, in both cnidarians (*e.g.*, sea anemones and jellyfish) and bilaterians (*e.g.*, worms, flies, and mammals) (2–5).

The 4-mer Phe-Met-Arg-Phe-amide (FMRFa) is a notable example. It is broadly expressed in neurons of invertebrate bilaterians, making it a commonly used marker of the nervous system in immunohistochemical experiments (6–8). Work in selected model bilaterians such as the ecdysozoans *Drosophila melanogaster* and *Caenorhabditis elegans* and the spiralian *Platynereis dumerilii* (an annelid) has begun identifying physiological responses mediated by FMRFa, cognate peptide/receptor pairs, and how these differ across different animals (9–12). Gastropod mollusks (slugs and snails—another group of spiralians) additionally possess an FMRFa-gated sodium channel (FaNaC), a receptor that mediates rapid neuronal and cardiac excitation upon FMRFa binding (13–15).

FaNaCs are members of the degenerin/epithelial sodium channel (DEG/ENaC) superfamily of trimeric sodium channels (14). In contrast to FaNaCs, the DEG/ENaC channels found in mammals are gated by increased proton concentrations (acid-sensing ion channels, ASICs), gated by bile acid (bile acid–gated channels), or are constitutively active (ENaCs) (16, 17). However, the binding of FMRFa or similar RFamides to ASICs has been shown to enhance proton-gated currents (18), perhaps offering a glimpse of their shared evolutionary history with FaNaCs and also raising interest in peptide-based pharmacological modulators of mammalian channels (15, 19). Knowledge of the molecular basis for FMRFa activity at its receptors would therefore offer insight into the role of neuropeptides and receptors in the evolution of bilaterian physiology and also enable the rational design of novel pharmacological modulators of mammalian receptors (20–22). Although previous studies showed that transplanting *Helisoma trivolvis* FaNaC (midmicromolar FMRFa potency) segments into *Helix aspersa* FaNaC (low-micromolar FMRFa potency) and *vice versa* alter FMRFa potency (23, 24), the molecular basis for FMRFa activity at its receptors is unknown.

We therefore sought to establish the molecular determinants of FMRFa activity in FaNaCs. Although previously described in only gastropod mollusks, we sought to characterize the FaNaC family in more depth and therefore considered closely related genes from other spiralians, such as annelids and platyhelminths, using phylogenetics, heterologous expression, and electrophysiological experiments. The resulting picture of the FaNaC family allowed us to

* For correspondence: Timothy Lynagh, tim.lynagh@uib.no.

© 2022 THE AUTHORS. Published by Elsevier Inc on behalf of American Society for Biochemistry and Molecular Biology. This is an open access article under the CC BY license (http://creativecommons.org/licenses/by/4.0/).

experimentally probe the molecular basis of FMRFa sensitivity in the broader family using site-directed mutagenesis. Together, our results identify key determinants of channel activation and modulation by FMRFa and other neuropeptides and offer insight into the evolution of the FaNaC family.

Results

Phylogenetic and experimental characterization of the FaNaC family

To identify the amino acid residues that determine FMRFa activity at FaNaCs, we considered comparing the amino acid sequences of previously characterized gastropod FaNaCs with other closely related channels of different function. However, gastropod FaNaCs comprise a narrow branch of the overarching DEG/ENaC superfamily, and sequence differences between this small number of channels and other DEG/ENaCs would be numerous, making the list of candidate amino acid residues long and impractical. We therefore sought a broader view of the FaNaC family and questioned if it extends beyond gastropods. To better estimate the breadth of the FaNaC family within the DEG/ENaC superfamily, we assembled DEG/ENaC sequences from numerous bilaterians and several other lineages and generated a maximum likelihood phylogeny of 544 nonredundant sequences (Fig. S1). Previously characterized FaNaCs from gastropods such as *H. aspersa* (14) appear in a well-supported clade, hereafter the "FaNaC branch" (Fig. 1*A*, *blue*). Notably, this branch also includes closely related sequences from other mollusks and from annelids and brachiopods, tentatively suggesting that FaNaCs occur in numerous spiralian animals. But the only nongastropod sequences from this branch that have been previously characterized are four from the annelid *Platyenereis dumerilii*, and when heterologously expressed, these did not respond to FMRFa, although one was activated by larger "Wamides," such as GWKQGASYSWa (25) ("MGIC *Platynereis dumerilii*", *pink* in Fig. 1*A*).

We next sought experimental evaluation of the broader FaNaC family seen in our phylogeny. To this end, we injected *Xenopus laevis* oocytes with cRNA of 20 uncharacterized genes from this or closely related branches (*asterisks* in Fig. 1*A*) and measured electrophysiological responses to FMRFa and a selection of neuropeptides encoded by the RFamide, FVRIamide, and Wamide propeptides from these animals (Fig. S2). To compare these with canonical gastropod FaNaCs, we performed similar experiments on *Aplysia kurodai* FaNaC (26). Genes from the cephalopod *Octopus bimaculoides*, the bivalve *Crassostrea gigas*, and the gastropod *Lottia gigantea* encoded FaNaCs similar to the gastropod *Aplysia* FaNaC, evident in large inward currents in response to both FMRFa and closely related peptides (Fig. 1, *B* and *C*). FMKFa and FLRFa, which in addition to FMRFa are encoded by the *Octopus* FMRFa propeptide (Fig. S2), activated larger currents than FMRFa at *Octopus* FaNaC, and FLRFa also activated slightly larger currents than FMRFa at *Crassostrea* FaNaC (Fig. 1, *B* and *C*). Interestingly, we observed that two genes from the annelid

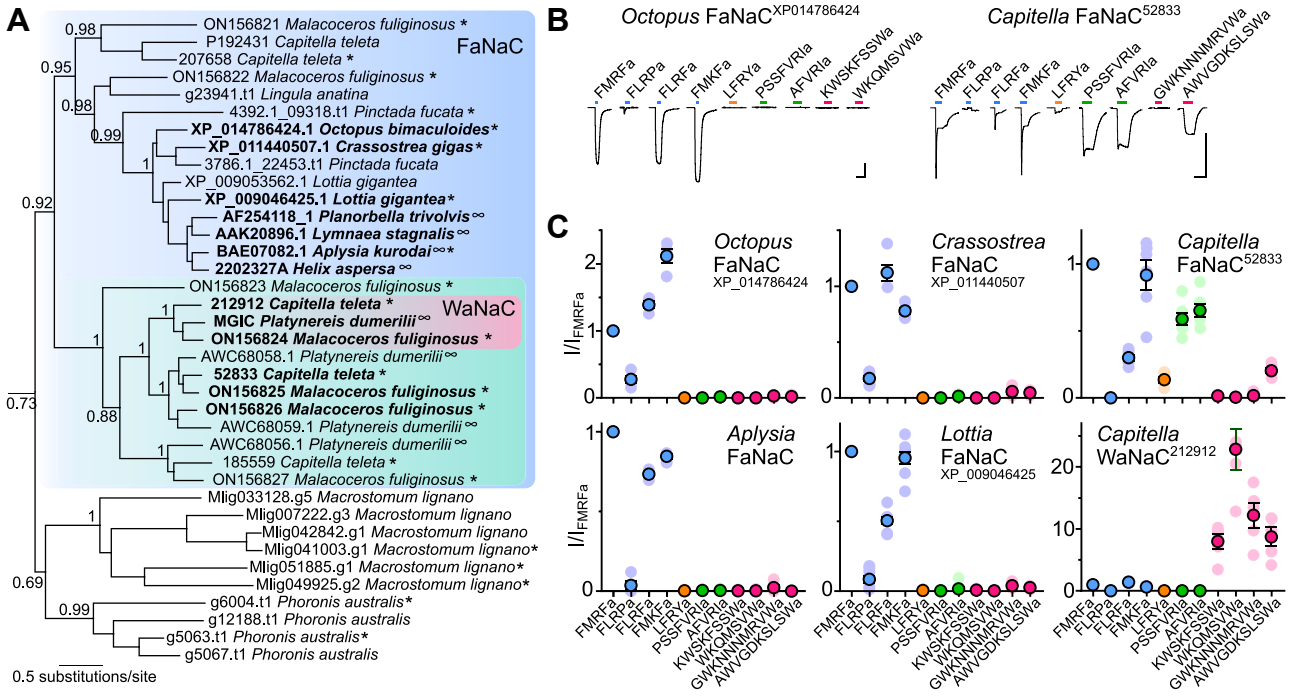

Figure 1. Phylogenetic and experimental characterization of the FaNaC family. *A*, FaNaC branch from DEG/ENaC phylogeny (full phylogeny in Fig. S1). *Genes tested here. ∞Genes tested elsewhere. Genes in bold encode peptide-gated channels. aLRT support for key branches is shown. *Blue background*, broader FaNaC family; *green background*, annelid-specific branch of FaNaCs with diverse ligand sensitivity; *pink background*, Wamide-activated channels (WaNaCs). *B*, example peptide-gated currents at *Xenopus* oocytes expressing indicated genes. All peptide applications 100 μM, except for some at *Capitella* FaNaC: FMRFa, FLRPa, FLRFa, and FMKFa (3 μM); LFRYa (30 μM). The scale bars represent x, 10 s; y, 5 μA. *C*, mean (± SEM) normalized current response to different peptides (concentrations as in (*B*)) at oocytes expressing indicated channels. *Lighter symbols* are individual data points, n = 4 to 7. FaNaC, FMRFa-gated sodium channel; FMRFa, Phe-Met-Arg-Phe-amide.

Capitella teleta, 52833 and 212912, also encoded channels gated by RFamides, FVRIamides, and/or Wamides (Fig. 1, *B* and *C*). This indicates that annelid genes from the FaNaC branch also encode FMRFa-gated and other peptide-gated channels. One of these, *Capitella* 52833, also showed small currents in response to LFRYa, a product of the RYamide propeptide from *Capitella* (Fig. 1, *B* and *C*). Together, these data describe a broader FaNaC family than previously realized and show that neuropeptides from FMRFa and/or other propeptides activate FaNaCs in various mollusks and in annelids.

We also tested three platyhelminth (*Macrostomum lignano*) and two phoronid (*Phoronis australis*) genes that appear in a small branch closely related to the FaNaC branch (lower clade in Fig. 1*A*). We injected oocytes with these RNAs either alone or in combination, in case of obligate heteromerization, but with these oocytes, we observed no response to FMRFa or YMRFa (from *Macrostomum* propeptide Mlig001796.g3), FVRIa (from *Phoronis* propeptide DN252244_c0_g1_i1), or GRTNNKNVFRWa or AYGSMPWa (both from *Macrostomum* propeptide Mlig032062.g1; n = 4–6). Consistent with the phylogenetic relationships we observe, this tentatively suggests that this branch is functionally distinct from the FaNaC branch. Whether this reflects the emergence of FaNaCs after the lineage to Annelida + Brachiopoda + Molluska split from the lineage to Platyhelminthes (and were lost in Phoronida) or whether FaNaCs emerged earlier and FMRFa sensitivity was lost in these platyhelminth and phoronid channels would require experiments on more channels. Furthermore, we cannot rule out that certain channels simply express poorly in our heterologous system, which could also relate to one mollusk and six annelid genes from the FaNaC branch itself, which showed no currents in response to FMRFa and other RFamides or to LFRYa, FVRIamides, or Wamides (n = 3–7; *asterisks*/nonbold font in Fig. 1*A*).

Activation of annelid FaNaCs by RFamides, FVRIamides, and Wamides contrasts with activation of mollusk FaNaCs by only RFamides (14, 25, 26) (Fig. 1*C*). We investigated this further by testing additional channels from this clade of annelid genes (*green* in Fig. 1*A*), also utilizing transcripts from another annelid, *Malacoceros fuliginosus*. *Capitella* 52833 and *Malacoceros* ON156825 and ON156826 were more potently activated by FMRFa than cognate Wamides and FVRIamides (Fig. 2, *A* and *B*), and we therefore refer to these channels as FaNaCs. The EC_{50} of FMRFa was 350 ± 150 nM (n = 7) at *Capitella* $FaNaC^{52833}$ and 230 ± 60 nM (n = 5) and 11 ± 3 μM (n = 8) at *Malacoceros* $FaNaC^{ON156825}$ and $FaNaC^{ON156826}$, respectively. In contrast, *Capitella* 212912 and *Malacoceros* ON156824 were more potently activated by cognate Wamides than by FMRFa and FVRIamides (Fig. 2, *A* and *B*), much like the previously characterized *Platynereis* MGIC from the same clade (*pink* in Fig. 1*A*, (25)), and we therefore refer to these as Wamide-gated sodium channels (WaNaCs). The AWVGDKSLSWa EC_{50} at *Capitella* $WaNaC^{212912}$ was 2 ± 0.2 μM (n = 8) and the KWGGNSRMWa EC_{50} at *Malacoceros* $WaNaC^{ON156824}$ was 340 ± 100 nM (n = 9). These results identify within the FaNaC branch a clade of annelid genes that evolved sensitivity to neuropeptides from other propeptides.

Comparison of FaNaCs with other DEG/ENaCs identifies molecular determinants of FMRFa sensitivity

With this broader view of FaNaC sequence and function, we returned to the aim of comparing amino acid sequences to identify amino acid residues that determine activation by FMRFa. An amino acid sequence alignment comparing the FaNaC family with other DEG/ENaCs, focusing on the putative extracellular and upper transmembrane domains of the protein, where ligand binding is likely to occur, identified 43

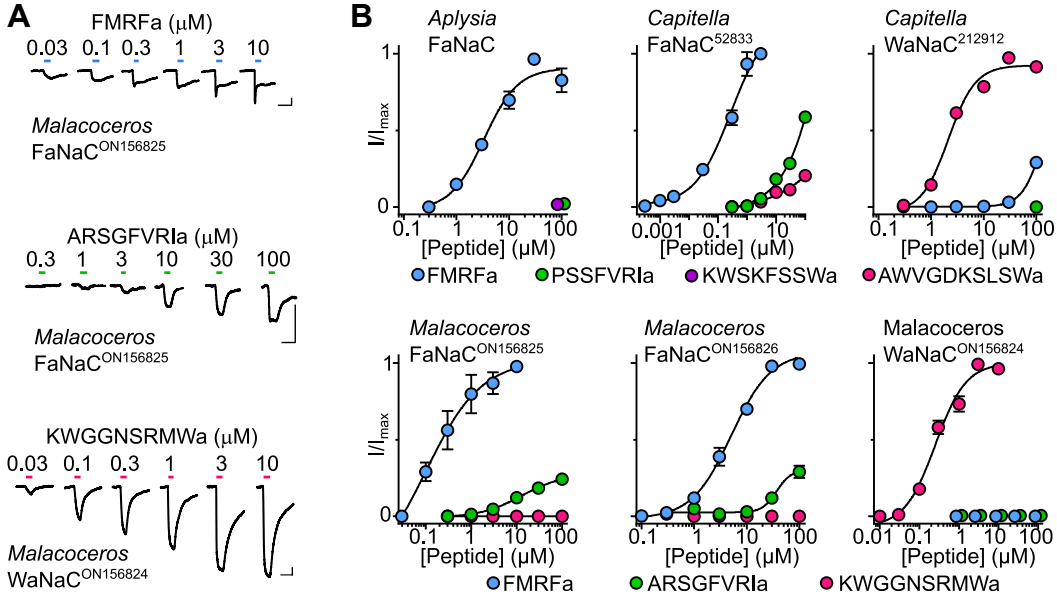

Figure 2. Neuropeptide sensitivity of different members of the FaNaC family. *A*, example currents in response to increasing concentrations of FMRFa, ARSGFVRIa, or KWGGNSRMWa at oocytes expressing indicated annelid (*Malacoceros fuliginosus*) channels. The scale bars represent x, 10 s; y, 1 μA. *B*, mean (± SEM, n = 4–5) normalized current responses to increasing concentrations of neuropeptides (as indicated) at FaNaCs and WaNaCs. FaNaC, FMRFa-gated sodium channel; FMRFa, Phe-Met-Arg-Phe-amide; WaNaC, Wamide-gated sodium channel.

amino acid residues that are reasonably conserved in FMRFa-gated channels but divergent in other DEG/ENaCs (Figs. 3*A* and S3). These 43 FaNaC-specific residues are spread throughout the extracellular domain, according to a homology-based structural model of *A. kurodai* FaNaC (Fig. 3*B*). We took *Aplysia* FaNaC as a representative FaNaC, and these 43 residues were individually (or together with one or two vicinal residues, for efficiency) mutated to an equivalent residue from channels not gated by FMRFa or, in two cases, to alanine if the equivalent position differed greatly among non-FMRFa-gated channels. This generated 30 *Aplysia* FaNaC mutants (*e.g.*, A319Q in Fig. 3*A*). FMRFa potency at WT and mutant channels was then measured in electrophysiological experiments. Current responses to 3 μM and 30 μM FMRFa were analyzed, giving an "$I_{3\ \mu M}/I_{30\ \mu M}$ ratio" of FMRFa potency, which was 0.64 ± 0.04 for WT (n = 14, Fig. 3, *C* and *D*), consistent with the FMRFa EC_{50} of 3.4 ± 0.4 μM (n = 5) from Figure 2*B*. Fifteen mutants showed unchanged or slightly increased FMRFa potency (*dark blue* in Fig. 3*D*), and eight mutants showed slightly decreased potency (*light blue* in Fig. 3*D*). The remaining seven mutants were not significantly activated by 3 or 30 μM FMRFa (Fig. 3*C*, *white* in Fig. 3*D*), indicating substantial decreases in potency and highlighting these seven positions as potential determinants of FMRFa activity at FaNaCs.

Of the seven mutants that showed a loss of FMRFa potency, two involved single substitutions (S184A and R324N), and the other five involved multiple substitutions (G270D/Y272L, I281T/S284D, S314F/G316T, S447V/W449F, and R529Q/L530V/N531S). We therefore clarified which of the substitutions underlay the functional effect in these five mutants by making additional single-substitution *Aplysia* FaNaC mutants. We did the same for Y230V/F231G, as this double-mutant showed the greatest decrease in FMRFa potency among the "moderate" mutants in Figure 3*D* (*light blue*). In five of these six cases, this clearly identified a single residue whose mutation decreases FMRFa potency (Fig. 4, *A* and *B*), namely F231G, I281T, G316T, S447V, and R529Q. In contrast, the single G270D and Y272L mutations only moderately decreased FMRFa potency (Fig. 4*B*), and we did not analyze these further. Full FMRFa concentration-response experiments on the loss-of-function single mutants revealed greater

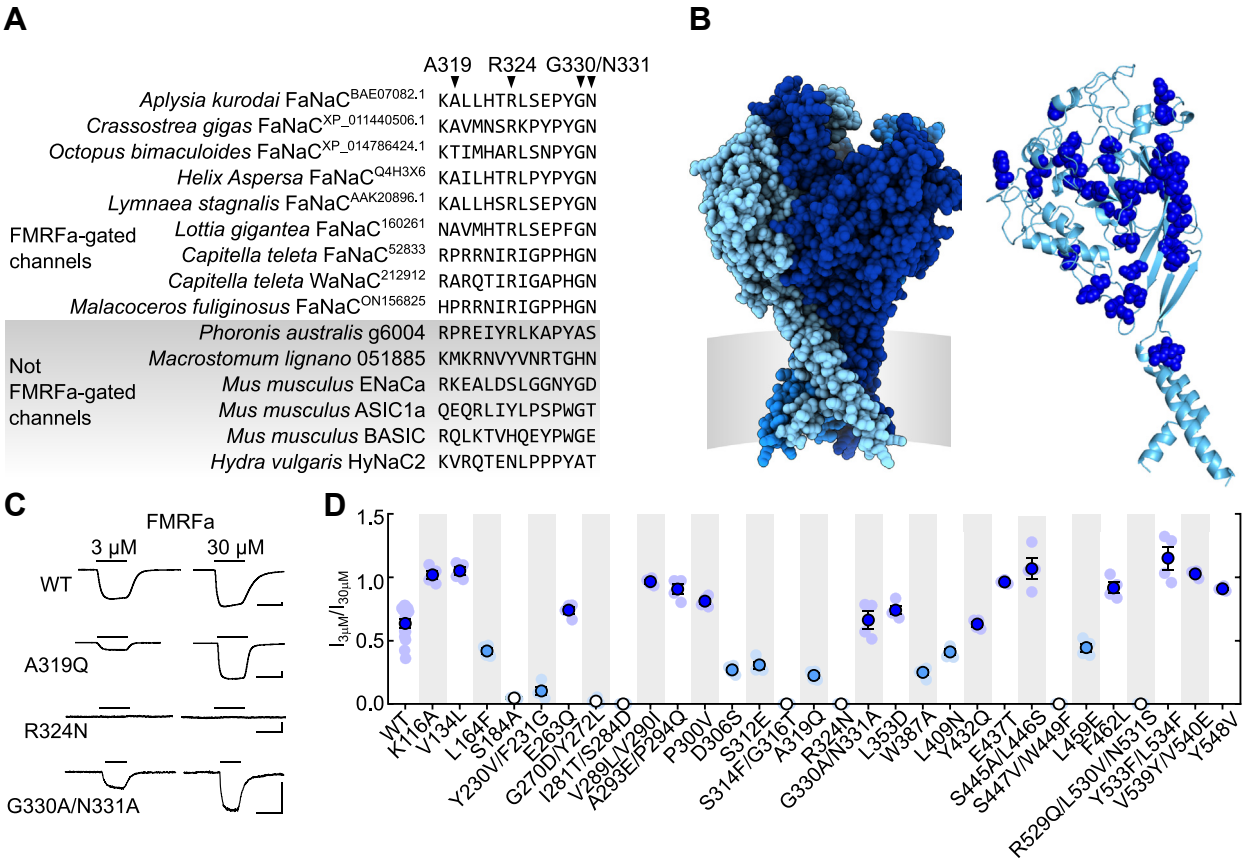

Figure 3. Comparative analysis of amino acid residues determining FMRFa sensitivity. *A*, part of amino acid sequence alignment comparing verified FMRFa-gated channels with other channels (complete alignment in Fig. S3). Examples of FaNaC-specific amino acid residues, that is, those that are conserved—either completely or in terms of physicochemical properties—in FaNaCs but different in other channels, are indicated by *arrowheads*. *B*, *left*, *Aplysia kurodai* FaNaC homology model. Different subunits in different shades of *blue*, approximate position of cell membrane in *gray*. *Right*, 43 FaNaC-specific amino acid residues (*dark blue spheres*) in a single subunit of model. *C*, example current responses to FMRFa at oocytes expressing WT or mutant *Aplysia kurodai* FaNaC channels. The scale bars represent x, 5 s; y, 1 μA. *D*, mean (± SEM) FMRFa potency (3 μM FMRFa-gated current amplitude/30 μM FMRFa-gated current amplitude: "$I_{3\ \mu M}/I_{30\ \mu M}$") was compared by one-way ANOVA with Dunnett's multiple comparisons test: *dark blue*, not significantly different to WT or significantly greater than WT; *light blue*, significantly less than WT ($p < 0.05$); *white*, not significantly different from zero. Individual data points shown as faint symbols, n = 3 to 14. FaNaC, FMRFa-gated sodium channel; FMRFa, Phe-Met-Arg-Phe-amide.

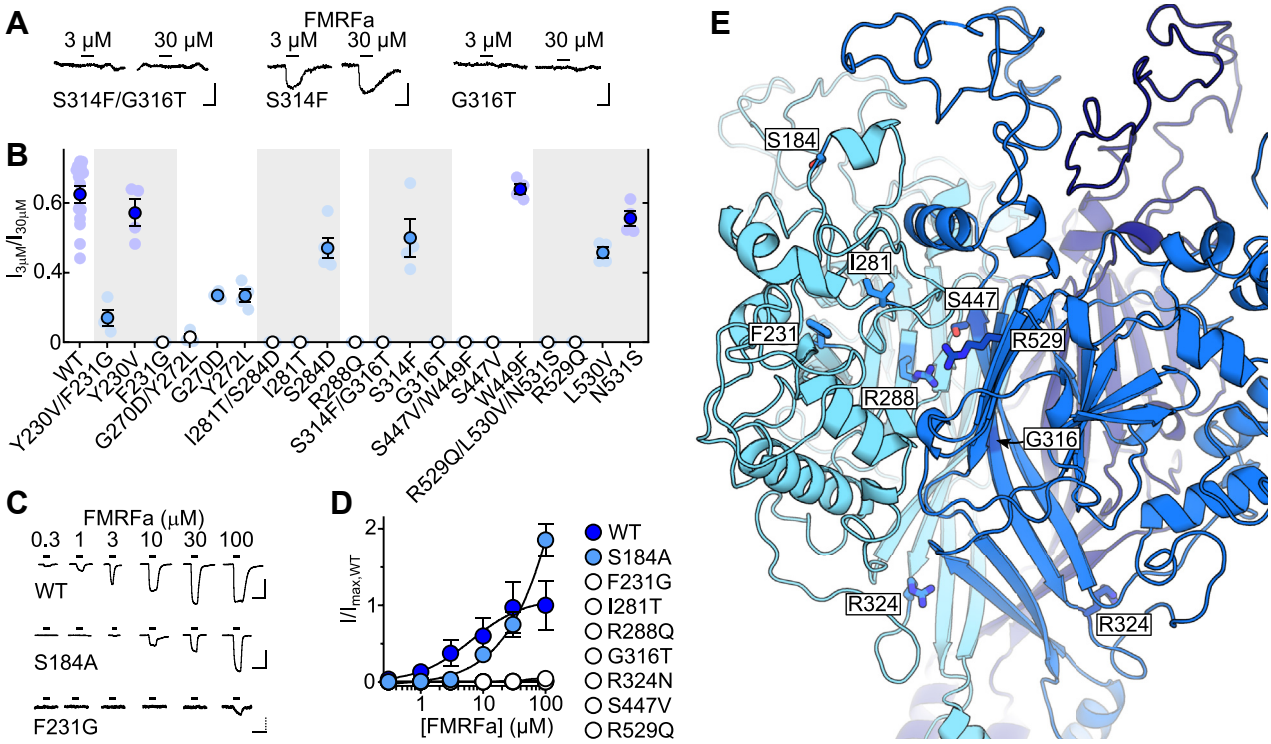

Figure 4. Isolation of individual determinants of FMRFa sensitivity in *Aplysia* FaNaC. *A*, example current responses to FMRFa at oocytes expressing mutant *Aplysia kurodai* FaNaC channels. The scale bars represent x, 5 s; y, 200 nA. *B*, mean (± SEM) FMRFa potency (3 μM FMRFa-gated current amplitude/30 μM FMRFa-gated current amplitude: "$I_{3\ \mu M}/I_{30\ \mu M}$"), WT repeated from Figure 3. *Dark blue*, not significantly different to WT; *light blue*, significantly less than WT ($p < 0.05$); *white*, not significantly different from zero. Individual data points as faint symbols, n = 4 to 14. *C*, example responses to increasing FMRFa concentrations at indicated *Aplysia* FaNaC mutants. The scale bars represent x, 10 s; y, 10 μA (WT and S184A) or 500 nA (F231G). *D*, mean (±SEM, n =3–6) normalized current amplitude in response to increasing FMRFa concentrations. Each individual data point was normalized to mean maximum current amplitude at WT (n = 3) on the same day. *E*, extracellular domain of *Aplysia* FaNaC homology model showing selected residues (*sticks*) at the interface of two adjacent subunits (one *cyan*, one *blue*). FaNaC, FMRFa-gated sodium channel; FMRFa, Phe-Met-Arg-Phe-amide.

decreases in FMRFa potency caused by F231G (small currents activated by 100 μM), I281T, G316T, R324N, S447V, and R529Q (negligible, if any, current activated by 100 μM) than by S184A (EC_{50} ≈ 30 μM, Fig. 4, *C* and *D*).

Seeking a potential explanation for the large effects of these mutations on FMRFa potency, we examined their location in a homology-based structural model of *Aplysia* FaNaC. Remarkably, F231, I281, G316, S447, and R529 all line a pocket at the interface of adjacent subunits in the extracellular domain of the channel (Fig. 4*E*). As the side chain of an additional residue, R288, auspiciously orients directly into this pocket, we also generated an R288Q mutant and observed that this mutation also abolished FMRFa potency (Fig. 4, *B* and *D*). We thus arrived at a list of seven major determinants of FMRFa activity in *Aplysia* FaNaC, F231, I281, R288, G316, S447, and R529, which line the extracellular pocket at the interface of adjacent subunits, and R324, which is in a loop immediately downstream of the β-strand containing G316 (Fig. 4*E*).

Molecular determinants of neuropeptide activity in mollusk and annelid FaNaCs and WaNaCs

We next tested if the close phylogenetic relationship of mollusk and annelid FaNaCs and WaNaCs is reflected in similar molecular determinants of neuropeptide activity at these channels. We mutated *Capitella* FaNaC^{52833} and *Capitella* WaNaC^{212912} at positions equivalent to the seven crucial residues identified in *Aplysia* FaNaC and tested mutant channels for responses to FMRFa or AWVGDKSLSWa (Fig. 5*A*). In *Capitella* FaNaC^{52833}, only R278Q and G306T mutations, equivalent to *Aplysia* FaNaC R288 and G316, abolished FMRFa-gated currents (*green* in Fig. 5*B*). In *Capitella* WaNaC^{212912}, R255Q, R291N, and R472Q mutations, equivalent to *Aplysia* FaNaC R288, R324, and R529, abolished AWVGDKSLSWa-gated currents (*pink* in Fig. 5*B*). Thus, the glycine residue in β-strand 9 (G316 in *Aplysia* FaNaC) seems crucial for FMRFa activation of FaNaCs; the arginine residue in β-strand 7 (R288 in *Aplysia* FaNaC) is crucial for neuropeptide activation of both FaNaCs and WaNaCs, and generally, arginine residues make a substantial contribution to channel sensitivity to neuropeptides.

Conserved determinants of neuropeptide sensitivity in distantly related DEG/ENaC channels

ASICs are members of the DEG/ENaC superfamily that are distantly related to FaNaCs (Fig. S1). ASICs are found in numerous bilaterians, including annelids, but are best described in mammals (27). Mammalian ASICs are closed at pH ≥7.4 and transiently activated by, for example, pH 5, but if resting channels are exposed to very small drops in pH, for example to pH 7, they enter a desensitized state and

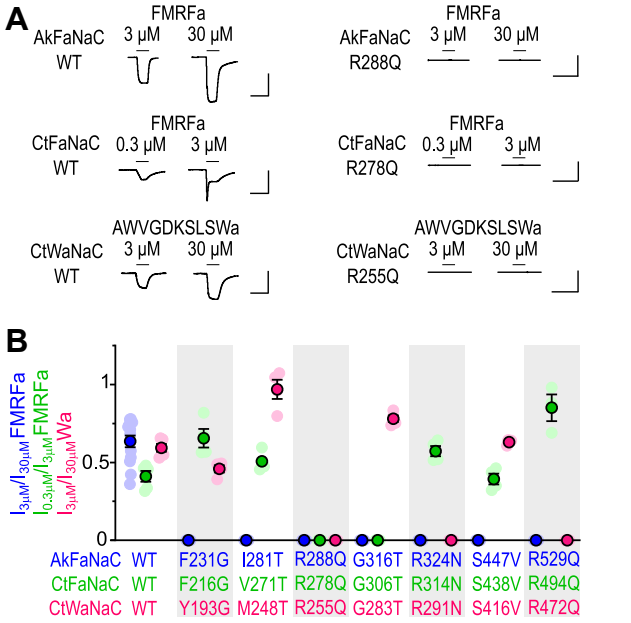

Figure 5. Determinants of neuropeptide activity in different FaNaCs and WaNaCs. *A*, example current responses to indicated neuropeptide at oocytes expressing WT or mutant *Aplysia* FaNaC (AkFaNaC), *Capitella* FaNaC[52833] (CtFaNaC), or *Capitella* WaNaC[212912] (CtWaNaC). The scale bars represent x, 10 s; y, 5 μA. *B*, average (± SEM, n = 4–5) FMRFa potency ($I_{3\ \mu M}/I_{30\ \mu M}$ at *Aplysia* FaNaC, $I_{0.3\ \mu M}/I_{3\ \mu M}$ at *Capitella* FaNaC) and AWVGDKSLSWa potency ($I_{3\ \mu M}/I_{30\ \mu M}$ at *Capitella* WaNaC), grouped according to the equivalent amino acid residue. FaNaC, FMRFa-gated sodium channel; WaNaC, Wamide-gated sodium channel.

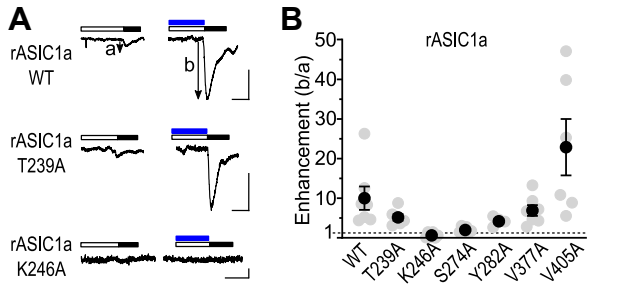

Figure 6. Determinants of FRRFa modulation of rat ASIC1a. *A*, pH 5.3 (*filled black bars*)-gated currents after preincubation in desensitizing pH (*unfilled bars*) alone or in 50 μM FRRFa (*blue bars*) at oocytes expressing WT or mutant rat ASIC1a (rASIC1a). The scale bars represent x, 10 s; y, 200 nA. Desensitizing pH described in Figure S4. *B*, mean (± SEM, n = 4–7) enhancement ($current_b/current_a$ from (*A*)) of desensitized current amplitude by 50 μM FRRFa at indicated rat ASIC1a mutants. ASIC, acid-sensing ion channel.

subsequently pH 5 activates little, if any, current (Fig. S4). However, in the presence of the synthetic FMRFa analog FRRFa, pH 7 induces less desensitization and subsequently pH 5 activates substantial current (19) (Fig. S4). FRRFa thus enhances ASICs, and finally, we questioned if this enhancement is determined by amino acid residues in a similar pocket to that identified in FaNaCs and WaNaCs.

Although we used mouse sequences in our earlier amino acid sequence analyses, we employed rat ASIC1a in our experiments because we had the clone in our laboratory, and rat and mouse ASIC1a differ at only one amino acid position in the intracellular domain. We measured FRRFa enhancement of pH-gated currents in rat ASIC1a WT and mutants carrying alanine substitutions at six of the seven positions addressed previously: T239A (equivalent to *Aplysia* FaNaC I281), K246A (FaNaC R288), S274A (FaNaC G316), Y282A (FaNaC R324), V377A (FaNaC S447), and V405A (FaNaC R529; full alignment in Fig. S3). We did not pursue ASIC1a G192 (FaNaC F231), as it was precisely the loss of a side chain in the *Aplysia* FaNaC F231G mutant that abolished FMRFa activity. At WT and four of the six mutant ASICs, FRRFa showed 4- to 23-fold enhancement of pH-gated currents (WT, 10 ± 3, n = 7; Fig. 6, *A* and *B*). Although not significantly less than WT (one-way ANOVA with Dunnett's multiple comparisons test), S274A mutant channels were enhanced only 2 ± 0.3-fold (n = 6), and K246A channels were not ostensibly enhanced at all (n = 6, Fig. 6, *A* and *B*). Thus, K246 in rat ASIC1a is crucial for FRRFa activity, much like the equivalent R288/R278/R255 residue in FaNaCs and WaNaCs is crucial for FMRFa/Wamide activity.

Discussion

We sought to establish the molecular determinants of FMRFa activity at FaNaCs by a comparative analysis of the FaNaC family. Our results lead to two major conclusions. Firstly, FaNaCs are found in multiple spiralian lineages, and in certain lineages, they have evolved sensitivity to other peptides. Secondly, a pocket in the extracellular domain of FaNaCs and other DEG/ENaCs contains several amino acid residues whose mutation abolishes FMRFa and/or other neuropeptide activity.

FaNaC evolution

Our combined phylogenetic and experimental analysis offers good evidence for a broader FaNaC family including mollusk, brachiopod, and annelid genes (*blue* in Fig. 1*A*). Within the FaNaC family, we see a well-supported clade of annelid genes encoding channels gated by FMRFa and/or other peptides from RFamide, FVRIamide, RYamide, and Wamide propeptides (*green* in Fig. 1*A*) and a well-supported clade of mollusk and brachiopod genes encoding channels gated by FMRFa and similar peptides from only the RFamide propeptide (upper clade in Fig. 1*A*). This suggests that the last common ancestor of annelids and mollusks had at least one gene encoding a FaNaC. At least two rounds of FaNaC gene duplications are evident in annelids, with one of the copies gaining sensitivity also to other neuropeptides such as Wamides, FVRIamides, and LFRYamide. Some of these genes, such as *Malacoceros* WaNaC[ON156824], have lost sensitivity to FMRFa.

More precise conclusions, especially on the early diversification of FaNaCs in annelids and mollusks, would need more extensive phylogenetic sampling and functional tests of the annelid and brachiopod genes (toward the *top* of Fig. 1*A*) that we were unable to characterize and that did not fall into well-supported clades. The fact that the closest relatives of the FaNaC family in our tree, genes from platyhelminths and phoronids, do not appear to form FMRF-gated channels, tentatively suggests that FaNaCs as we know them emerged in an early ancestor of annelids + brachiopods + mollusks, after this lineage split from the lineage to platyhelminths. However, this interpretation suffers from (a) poor branch support and

(b) the possibility that genes we have not tested—in the platyhelminth/phoronid clade and in various other clades—could form FMRFa-gated channels. The fact that such diverse DEG/ENaCs as FaNaCs, ASICs, and hydrozoan peptide-gated sodium channels are sensitive to RFamides, whether activated or only modulated, also suggests that peptide-sensitive channels may be "hiding" in other branches of the DEG/ENaC tree.

Molecular determinants of FMRFa sensitivity in FaNaCs and other DEG/ENaCs

Our results identify a conserved arginine residue in FaNaCs and WaNaCs that is required for channel activation by FMRFa and Wamides. Six other conserved FaNaC/WaNaC residues also contribute to FMRFa or Wamide potency but only in certain channels. According to our homology-based structural model of *Aplysia* FaNaC, six of the seven determinants of potency line a pocket formed by the interface of adjacent subunits in the channel's extracellular domain. The crucial arginine side chain (R288 in *Aplysia* FaNaC) orients from the left subunit into the middle of the pocket.

Knowledge of the structure of DEG/ENaCs derives mostly from X-ray crystallography of chick ASIC1 (28), on which our *Aplysia* FaNaC model is based. Our model suffers from low-sequence identity with the template (21%) and long loops between extracellular β-strands relative to the template. Therefore, the location and orientation of F231 and I281 in our model is questionable. However, the location of R288, G316, S447, and R529 in β-strands forming the interfacial pocket, and even R324 in a "thumb domain" loop downstream of G316 (28), seems more reliable: throughout the DEG/ENaC family these segments are more conserved, have less indels, and are also close to conserved cysteine residues that stabilize structure *via* disulfide bonds (Fig. S3). The crucial arginine, in particular, may have a similar orientation and functional role in neuropeptide sensitivity in diverse DEG/ENaCs. It was not identified in our initial comparative analysis because rather than being FaNaC-specific, a basic arginine or lysine residue occurs at this position in numerous DEG/ENaCs (Fig. S3). Our observation that FRRFa enhancement of rat ASIC1a was abolished by the K246A mutation is consistent with a conserved role of this basic residue in neuropeptide sensitivity (but see later).

The few previous studies that probed the determinants of FMRFa sensitivity in FaNaCs were limited by our understanding of the FaNaC family at the time. These mutagenesis studies addressed the relatively small difference between two snail FaNaCs, from *Helix aspersa* (EC_{50} = 3 μM) and *Helisoma trivolvis* (EC_{50} = 100 μM). Although the substitution of a 32 aa segment (including the residue equivalent to *Aplysia* FaNaC F231) from *Helix* FaNaC into *Helisoma* FaNaC conferred 3 μM FMRFa sensitivity on the latter (23), and several *Helisoma*-oriented substitutions in *Helix* FaNaC caused moderate decreases in FMRFa potency (24), such *Helix*-specific amino acid residues are not necessarily correlated with FMRFa sensitivity throughout the broader FaNaC family and are unlikely to account for the substantial functional differences between FaNaCs and other channels. These functional differences instead seem to derive from the seven determinants identified presently. Indeed, with knowledge of these seven determinants, we revisited the sequences of genes that did not respond to neuropeptides when expressed in oocytes in our experiments (*asterisks*/nonbold font in Fig. 1*A*). The mollusk *Pinctada fucata* 4392.1_09318.t1 sequence differs from *bona fide* FaNaCs at most of the key positions, with (*Aplysia* FaNaC numbering) F231L, I281Y, R288T, G316A, and R324Y differences. Certain annelid sequences from both major branches of the FaNaC family (Fig. 1*A*, *blue* and *green*) that did not form peptide-gated channels also differed at some of these key positions, including *Malacoceros fuliginosus* ON156821 (R288V, G316A, and R324K) and ON156823 (F231L and I281S). This tentatively suggests that those channels express but do not respond to FMRFa or similar peptides due to divergence at these amino acid positions.

Several studies have considered RFamide modulation of ASICs, given the therapeutic potential of peptide modulators of vertebrate ASICs. Rat ASIC1a S274 (equivalent to *Aplysia* FaNaC G316), whose mutation to alanine abolished FRRFa enhancement of ASIC1a in our hands, was previously implicated in the different levels of FMRFa enhancement of rodent compared to human ASIC1a (19). Rat ASIC1a S274 is close to several other residues whose mutation in human ASIC1a decreases FRRFa enhancement, although these other residues line a vestibule formed just above the channel pore, enclosed by the three subunits of the trimeric channel (29), rather than the more external pocket we describe presently. Similarly, RPRFa enhancement of rat ASIC3 is drastically reduced by mutations in this same vestibule, also called the nonproton ligand-sensing domain (30). This raises the possibility that the rat ASIC1a K246A mutation, which abolished FRRFa enhancement in our hands, could do so due to an indirect involvement of K246 in enhancement of ASIC1a upon RFamide binding to a different site. This would also mean that distinct RFamide-binding sites occur throughout the DEG/ENaC family. Whether hydrozoan peptide-gated sodium channels (31), which are more closely related to ASICs than FaNaCs in sequence (Fig. S1), depend more on the external extracellular pocket or on the central vestibule for their activation by hydrozoan RFamides remains to be explored.

Potential roles of extracellular pocket in neuropeptide activity

Residues in the extracellular pocket of FaNaC could determine peptide activity by forming the binding site for peptides or by mediating conformational changes required for channel opening in response to peptide binding elsewhere. Our experiments do not distinguish between these possibilities, but the interfacial, extracellular location of the pocket is reminiscent of binding sites in other ligand-gated ion channel families. In trimeric ATP-gated channels, phylogenetically distinct from DEG/ENaCs but structurally similar and with a similarly sized agonist, ATP binds in the extracellular domain at the interface of adjacent subunits, causing conformational changes that lead to channel opening (32). Similarly, in pentameric ligand-gated

ion channels, such as excitatory nicotinic acetylcholine receptors, agonist binding to the interface of adjacent subunits causes the left subunit to close around the agonist pulling the lower parts of the receptor into an open channel state (33). The remaining ligand-gated ion channel superfamily of tetrameric ionotropic glutamate receptors is distinct, in that their structure consists of an extracellular agonist-binding domain contained within each subunit, derived from a soluble substrate-binding protein in bacteria (34).

We speculate that RFamides and Wamides bind to the interfacial pocket, where the two aromatics of the neuropeptide could form hydrophobic interactions with F231 or I281 or cation–π interactions with R288 or R529. Similarly, the basic arginine or lysine side chain in most of these neuropeptides could engage with hydrophilic moieties in the channel pocket, such as the S447 side chain or main chain carbonyls from the loops at the top of the pocket, or form cation–π interactions either with the receptor or within the neuropeptide itself. Such interactions are exemplified by the binding mode at other channels of certain peptide toxins and synthetic peptides, some of which, like FMRFa, contain arginine and aromatic side chains in close proximity (35–37). Foreseeably, conformational changes in this part of the extracellular domain of FaNaCs could be mechanically coupled to channel gating *via* the β-strand containing G316 and, slightly downstream, the loop containing R324, a loop previously implicated in channel gating of diverse DEG/ENaCs (38, 39).

Outlook

As the molecular basis for FMRFa activity at its receptors was previously unknown, we employed a combination of phylogenetics and experimental dissection to investigate FMRFa activity at FaNaCs. In addition to identifying the molecular determinants of FMRFa activity at both gastropod and annelid FaNaCs and WaNaCs, this approach also disentangled evolutionary relationships between these FaNaC family members. Furthermore, it uncovered a molecular and functional link between FaNaCs and more distantly related ASICs. These results enable better prediction of function from sequence, offer numerous spiralian RFamide-sensitive channels for investigation as potential targets for marine predators employing RFamide venoms (40), and offer a springboard for future studies addressing DEG/ENaC evolution and neuropeptide-binding sites in detail.

Experimental procedures

Sequence assembly and phylogenetic analysis

To investigate the presence of FMRFa-sensitive channels throughout the metazoans, DEG/ENaC amino acid sequences were sought from four mollusks (*C. gigas*, *O. bimaculoides*, *P. fucata*, and *L. gigantea*), four cnidarians (*Aurelia aurita*, *Hydra vulgaris*, *Nematostella vectensis*, and *Stylophora pistillata*), four annelids (*C. teleta*, *Platynereis dumerili*, *M. fuliginosus*, and *Helobdella robusta*), one phoronid (*P. australis*), one brachiopod (*Lingula anatina*), one nemertean (*Notospermus geniculatus*), one rotifer (*Branchionus plicatilis*), one platyhelminth (*M. lignano*), one arthropod (*Araneus ventricosus*), one priapulid (*Priapulus caudatus*), two chordates (*Branchiostoma belcheri* and *Homo sapiens*), two echinoderms (*Acanthaster planci* and *Strongylocentrotus purpuratus*), two poriferans (*Amphimedon queenslandica* and *Oscarella carmela*), one ctenophore (*Mnemiopsis leidyi*), and one hemichordate (*Ptychodera flava*). Sequences were obtained through BlastP using the *A. kurodai* FaNaC amino acid sequence (NCBI BAE07082.1) in JGI Capca1 genome (*C. teleta*, https://mycocosm.jgi.doe.gov/pages/blast-query.jsf?db=Capca1 (41)), OIST Marine Genomics Unit (*P. fucata, P. australis*, *N. geniculatus*, and *A. aurita*, https://marinegenomics.oist.jp/gallery), *M. lignano* genome initiative (*M. lignano*, http://www.macgenome.org/blast/index.html), Compagen Japan (*O. carmela*, http://203.181.243.155/blast.html), our own *M. fuliginosus* transcriptome resources (42), or NCBI (for all others, https://blast.ncbi.nlm.nih.gov). After an initial alignment using MAFFT v 7.450 in Geneious Prime (Geneious), removal of >90% identical, redundant sequences and removal of obviously incomplete sequences, sequences were realigned with MAFFT and poor-aligning segments and sequences larger than 1000 aa or shorter than 300 aa were removed. The result was an alignment of 544 sequences with 9829 amino acid positions (or gaps). This alignment was used to generate a maximum likelihood tree with PhyML (http://www.atgc-montpellier.fr/phyml/ (43)) using a VT + G substitution model chosen by Smart Model Selection in PhyML (44). Branch support was estimated through aLRT SH-like based method (43).

Molecular biology, chemicals, and peptides

Sequences chosen for complementary DNA (cDNA) synthesis, cRNA transcription and expression were *C. gigas* XM_011442205.2, *O. bimaculoides* XM_014930938.1, *L. gigantea* XM_009055314.1_160261, *P. fucata* pfu_aug2.0_4392.1_09318.t1, *C. teleta* Capca1_207658, Capca1_52833 (alternative splice variant, Capca1_191096, using fgenesh *ab initio* models was used), Capca1_185559, and Capca1_212912, *M. fuliginosus* ON156821, ON156822, ON156823, ON156824, ON156825, ON156826, and ON156827, *M. lignano* Mlig049925.g2, Mlig051885.g1, and Mlig041003.g1, and *P. australis* g6004.t1 and g5063.t1. These were selected based on their position in the FaNaC or adjacent clade (Fig. 1*A*) and to a lesser extent, which animal lineage they represent. *A. kurodai* BAE07082.1 (*Aplysia* FaNaC) cDNA in a modified pSP64 vector was provided by Prof. Yasuo Furukawa, Hiroshima University, Japan. *Rattus norvegicus* NP_077068.1 (rat ASIC1a) in the pRSSP6009 vector was provided by Prof. Stefan Gründer, RWTH Aachen University. cDNA for the other sequences was commercially synthesized and subcloned (Genscript) between SalI and BamHI sites in a pSP64 (polyA) vector (Promega) modified based on (45) and containing a C-terminal cMyc tag (Supporting Text).

Site-directed mutagenesis was performed with custom designed primers (Merck) and PCR with Phusion High-Fidelity DNA polymerase (Thermo Fisher Scientific) following the supplier's PCR protocol and using primers designed according

to (46). All sequences—mutant and WT—were confirmed by Sanger sequencing of the full insert (Genewiz). cDNAs were linearized with EcoRI, Pdil, or XbaI (ThermoFisher Scientific), and cRNA was transcribed with the mMESSAGE mMACHINE SP6 Transcription Kit (Thermo Fisher Scientific).

Peptides were custom synthesized by Genscript, mass was confirmed by electrospray ionization mass spectrometry, ≥95% purity confirmed by reversed-phase HPLC, and TFA replaced with acetic acid. Salts and other standard chemicals were purchased from Merck.

Heterologous expression and electrophysiology

Defolliculated stage V/VI oocytes from *X. laevis* were commercially acquired (Ecocyte Bioscience) and stored at 18 °C in 50% (in water) Leibovitz's L-15 medium (Gibco) supplemented with additional 0.25 mg/ml gentamicin, 1 mM L-glutamine, and 15 mM Hepes, pH 7.6. Oocytes were injected with 2 ng cRNA (WT or mutant *Aplysia* FaNaC) and 2 to 60 ng cRNA (WT *C. gigas* XM_011442205.2, *O. bimaculoides* XM_014930938.1, *L. gigantea* XM_009055314.1_160261, *P. fucata* pfu_aug2.0_4392.1_09318.t1, *C. teleta* Capca1_207658, Capca1_52833, Capca1_185559, and Capca1_212912, *M. lignano* Mlig049925.g2, Mlig051885.g1, and Mlig041003.g1, *P. australis* g6004.t1 and g5063.t1 and *R. norvegicus* NP_077068.1 (rat ASIC1a) and respective mutants). Two-electrode voltage clamp experiments were performed 1 to 3 days after injection. The oocyte was placed in an RC-3Z bath (Warner Instruments) and bath solution (NaCl: 96 mM, KCl: 2 mM, $CaCl_2$: 1.8 mM, $MgCl_2$: 1 mM, Hepes: 5 mM; pH: 7.5) was perfused continuously and rapidly switched to bath solution containing peptide ligands *via* the VCS-8-pinch valve control perfusion system (Warner Instruments). In initially determining peptide sensitivity of various channels, all peptides were applied at 100 μM, except at *Capitella* $FaNaC^{52833}$, which showed slow washout of FMRFa-gated current and was therefore exposed to 3 μM FMRFa, FLRPa, FLRFa, and FMKFa, 30 μM LFRYa, and 100 μM PSSFVRIa, GWKNNNMRVWa, and AWVGDKSLSWa. Peptides were applied at varying concentrations between 30 nM and 100 μM for concentration-response experiments. The oocytes were clamped at −40 mV for rat ASIC1a experiments and −60 mV for all others with an Oocyte Clamp OC-725C amplifier (Warner Instruments), LIH 8 + 8 digitizer (HEKA Elektronik) at 0.5 or 1 KHz sampling and 100 Hz filtering. Current recordings were analyzed in Clampfit 11.1 (Molecular Devices).

After retrieving current amplitude from pClamp, all data analyses were performed in Prism v9 (GraphPad Software). For peptide or proton concentration-response data, peak current amplitude was plotted against peptide concentrations or pH and fitted with the Hill equation for each recording. These were averaged to give the reported means ± SEM in the main text. For display in figures, a single fit to the average normalized responses (±SEM) is shown. Multiple comparisons were made with one-way ANOVA with Dunnett's comparison to a control value (*e.g.*, comparing with WT) or with Tukey's test for multiple comparisons.

FaNaC structural model

A rudimentary structural model of *A. kurodai* FaNaC was generated by uploading its protein sequence to the Swiss model server (47), which suggested chick ASIC1a structure PDB 4NYK (48) as an appropriate template and generated a pdb file, which is visualized in Figures 3 and 4 using PyMOL software (Schrödinger).

Data availability

DNA sequences are included in supporting information. Amino acid sequence alignment and maximum likelihood tree are available at lynaghlab.com/resources. Electrophysiological data points are shown where possible and are available from the corresponding author on request.

Supporting information—This article contains supporting information (42, 45).

Acknowledgments—We are grateful to Prof. Yasuo Furukawa (Hiroshima University, Japan) for the *Aplysia kurodai* FaNaC clone, Prof. Stefan Gründer (RWTH Aachen University, Germany) for the rat ASIC1a clone, and to Dr Josep Martí-Solans (University of Bergen, Norway) and Dr Valeria Kalienkova (University of Groningen, Netherlands) for helpful discussions on the manuscript.

Author contributions—T. L. conceptualization; M. D. and T. L. methodology; M. D. and T. L. formal analysis; M. D. and H. H. investigation; H. H. resources; M. D. and T. L. writing–original draft; M. D., H. H., and T. L. writing–review & editing; M. D. and T. L. visualization; T. L. supervision.

Funding and additional information—This work was supported by The Research Council of Norway, project number 234817.

Conflict of interest—The authors declare that they have no conflicts of interest with the contents of this article.

Abbreviations—The abbreviations used are: ASIC, acid-sensing ion channel; cDNA, complementary DNA; DEG/ENaC, degenerin/epithelial sodium channel; FaNaC, FMRFa-gated sodium channel; FMRFa, 4-mer Phe-Met-Arg-Phe-amide; WaNaC, Wamide-gated sodium channel.

References

1. Elphick, M. R., Mirabeau, O., and Larhammar, D. (2018) Evolution of neuropeptide signalling systems. *J. Exp. Biol.* **221**, jeb151092
2. Dale, H. H. (1909) The action of extracts of the pituitary body. *Biochem. J.* **4**, 427–447
3. McFarlane, I. D., Graff, D., and Grimmelikhuijzen, C. J. P. (1987) Excitatory actions of antho-RFamide, an anthozoan neuropeptide, on muscles and conducting systems in the sea anemone calliactis parasitica. *J. Exp. Biol.* **133**, 157–168
4. Nichols, R. (2003) Signaling pathways and physiological functions of Drosophila melanogaster FMRFamide-related peptides. *Annu. Rev. Entomol.* **48**, 485–503
5. Price, D. A., and Greenberg, M. J. (1977) Structure of a molluscan cardioexcitatory neuropeptide. *Science* **197**, 670–671
6. Achatz, J. G., and Martinez, P. (2012) The nervous system of Isodiametra pulchra (Acoela) with a discussion on the neuroanatomy of the Xenacoelomorpha and its evolutionary implications. *Front. Zool.* **9**, 27

7. Starunov, V. V., Voronezhskaya, E. E., and Nezlin, L. P. (2017) Development of the nervous system in Platynereis dumerilii (Nereididae, Annelida). *Front. Zool.* **14**, 27
8. White, K., Hurteau, T., and Punsal, P. (1986) Neuropeptide-FMRFamide-like immunoreactivity in Drosophila: development and distribution. *J. Comp. Neurol.* **247**, 430–438
9. Bauknecht, P., and Jékely, G. (2015) Large-scale combinatorial deorphanization of Platynereis neuropeptide GPCRs. *Cell Rep.* **12**, 684–693
10. Cazzamali, G., and Grimmelikhuijzen, C. J. P. (2002) Molecular cloning and functional expression of the first insect FMRFamide receptor. *Proc. Nat. Acad. Sci. U. S. A.* **99**, 12073–12078
11. Nässel, D. R., and Winther, Å. M. E. (2010) Drosophila neuropeptides in regulation of physiology and behavior. *Prog. Neurobiol.* **92**, 42–104
12. Oranth, A., Schultheis, C., Tolstenkov, O., Erbguth, K., Nagpal, J., Hain, D., *et al.* (2018) Food sensation modulates locomotion by dopamine and neuropeptide signaling in a distributed neuronal network. *Neuron* **100**, 1414–1428.e10
13. Cottrell, G. A., Green, K. A., and Davies, N. W. (1990) The neuropeptide Phe-Met-Arg-Phe-NH2 (FMRFamide) can activate a ligand-gated ion channel in Helix neurons. *Pflügers Arch.* **416**, 612–614
14. Lingueglia, E., Champigny, G., Lazdunski, M., and Barbry, P. (1995) Cloning of the amiloride-sensitive FMRFamide peptide-gated sodium channel. *Nature* **378**, 730–733
15. Perry, S. J., Straub, V. A., Schofield, M. G., Burke, J. F., and Benjamin, P. R. (2001) Neuronal expression of an FMRFamide-gated Na+ channel and its modulation by acid pH. *J. Neurosci.* **21**, 5559–5567
16. Kellenberger, S., and Schild, L. (2015) International Union of Basic and Clinical Pharmacology. XCI. Structure, function, and pharmacology of acid-sensing ion channels and the epithelial Na+ channel. *Pharmacol. Rev.* **67**, 1–35
17. Wiemuth, D., Assmann, M., and Grunder, S. (2014) The bile acid-sensitive ion channel (BASIC), the ignored cousin of ASICs and ENaC. *Channels (Austin)* **8**, 29–34
18. Askwith, C. C., Cheng, C., Ikuma, M., Benson, C., Price, M. P., and Welsh, M. J. (2000) Neuropeptide FF and FMRFamide potentiate acid-evoked currents from sensory neurons and proton-gated DEG/ENaC channels. *Neuron* **26**, 133–141
19. Sherwood, T. W., and Askwith, C. C. (2008) Endogenous arginine-phenylalanine-amide-related peptides alter steady-state desensitization of ASIC1a. *J. Biol. Chem.* **283**, 1818–1830
20. Heusser, S. A., and Pless, S. A. (2021) Acid-sensing ion channels as potential therapeutic targets. *Trends Pharmacol. Sci.* **42**, 1035–1050
21. Jekely, G. (2021) The chemical brain hypothesis for the origin of nervous systems. *Philos. Trans. R. Soc. Lond. B Biol. Sci.* **376**, 20190761
22. Mousley, A., Marks, N. J., and Maule, A. G. (2004) Neuropeptide signalling: a repository of targets for novel endectocides? *Trends Parasitol.* **20**, 482–487
23. Cottrell, G. A. (2005) Domain near TM1 influences agonist and antagonist responses of peptide-gated Na+ channels. *Pflugers Arch.* **450**, 168–177
24. Niu, Y.-Y., Yang, Y., Liu, Y., Huang, L.-D., Yang, X.-N., Fan, Y.-Z., *et al.* (2016) Exploration of the peptide recognition of an amiloride-sensitive FMRFamide peptide-gated sodium channel. *J. Biol. Chem.* **291**, 7571–7582
25. Schmidt, A., Bauknecht, P., Williams, E. A., Augustinowski, K., Grunder, S., and Jekely, G. (2018) Dual signaling of Wamide myoinhibitory peptides through a peptide-gated channel and a GPCR in Platynereis. *FASEB J.* **32**, 5338–5349
26. Furukawa, Y., Miyawaki, Y., and Abe, G. (2006) Molecular cloning and functional characterization of the Aplysia FMRFamide-gated Na+ channel. *Pflugers Arch.* **451**, 646–656
27. [preprint] Martí-Solans, J., Børve, A., Bump, P., Hejnol, A., and Lynagh, T. (2022) Peripheral and central employment of acid-sensing ion channels during early bilaterian evolution. *bioRxiv*. https://doi.org/10.1101/2022.03.17.484724
28. Jasti, J., Furukawa, H., Gonzales, E. B., and Gouaux, E. (2007) Structure of acid-sensing ion channel 1 at 1.9 A resolution and low pH. *Nature* **449**, 316–323
29. Bargeton, B., Iwaszkiewicz, J., Bonifacio, G., Roy, S., Zoete, V., and Kellenberger, S. (2019) Mutations in the palm domain disrupt modulation of acid-sensing ion channel 1a currents by neuropeptides. *Sci. Rep.* **9**, 2599
30. Reiners, M., Margreiter, M. A., Oslender-Bujotzek, A., Rossetti, G., Gründer, S., and Schmidt, A. (2018) The conorfamide RPRFa stabilizes the open conformation of acid-sensing ion channel 3 via the nonproton ligand–sensing domain. *Mol. Pharmacol.* **94**, 1114–1124
31. Assmann, M., Kuhn, A., Dürrnagel, S., Holstein, T. W., and Gründer, S. (2014) The comprehensive analysis of DEG/ENaC subunits in hydra reveals a large variety of peptide-gated channels, potentially involved in neuromuscular transmission. *BMC Biol.* **12**, 84
32. Hattori, M., and Gouaux, E. (2012) Molecular mechanism of ATP binding and ion channel activation in P2X receptors. *Nature* **485**, 207–212
33. Noviello, C. M., Gharpure, A., Mukhtasimova, N., Cabuco, R., Baxter, L., Borek, D., *et al.* (2021) Structure and gating mechanism of the alpha7 nicotinic acetylcholine receptor. *Cell* **184**, 2121–2134.e13
34. Wo, Z. G., and Oswald, R. E. (1995) Unraveling the modular design of glutamate-gated ion channels. *Trends Neurosci.* **18**, 161–168
35. Lynagh, T., Kiontke, S., Meyhoff-Madsen, M., Gless, B. H., Johannesen, J., Kattelmann, S., *et al.* (2020) Peptide inhibitors of the α-cobratoxin–nicotinic acetylcholine receptor interaction. *J. Med. Chem.* **63**, 13709–13718
36. Rahman, M. M., Teng, J., Worrell, B. T., Noviello, C. M., Lee, M., Karlin, A., *et al.* (2020) Structure of the native muscle-type nicotinic receptor and inhibition by snake venom toxins. *Neuron* **106**, 952–962.e5
37. Yen, T. J., Lolicato, M., Thomas-Tran, R., Du Bois, J., and Minor, D. L., Jr. (2019) Structure of the saxiphilin:saxitoxin (STX) complex reveals a convergent molecular recognition strategy for paralytic toxins. *Sci. Adv.* **5**, eaax2650
38. Li, T., Yang, Y., and Canessa, C. M. (2009) Interaction of the aromatics Tyr-72/Trp-288 in the interface of the extracellular and transmembrane domains is essential for proton gating of acid-sensing ion channels. *J. Biol. Chem.* **284**, 4689–4694
39. Shi, S., Ghosh, D. D., Okumura, S., Carattino, M. D., Kashlan, O. B., Sheng, S., *et al.* (2011) Base of the thumb domain modulates epithelial sodium channel gating. *J. Biol. Chem.* **286**, 14753–14761
40. Terlau, H., and Olivera, B. M. (2004) Conus venoms: a rich source of novel ion channel-targeted peptides. *Physiol. Rev.* **84**, 41–68
41. Simakov, O., Marletaz, F., Cho, S.-J., Edsinger-Gonzales, E., Havlak, P., Hellsten, U., *et al.* (2013) Insights into bilaterian evolution from three spiralian genomes. *Nature* **493**, 526–531
42. Kumar, S., Tumu, S. C., Helm, C., and Hausen, H. (2020) The development of early pioneer neurons in the annelid Malacoceros fuliginosus. *BMC Evol. Biol.* **20**, 117
43. Guindon, S., Dufayard, J.-F., Lefort, V., Anisimova, M., Hordijk, W., and Gascuel, O. (2010) New algorithms and methods to estimate maximum-likelihood phylogenies: assessing the performance of PhyML 3.0. *Syst. Biol.* **59**, 307–321
44. Lefort, V., Longueville, J.-E., and Gascuel, O. (2017) SMS: smart model selection in PhyML. *Mol. Biol. Evol.* **34**, 2422–2424
45. Krieg, P. A., and Melton, D. A. (1984) Functional messenger RNAs are produced by SP6 *in vitro* transcription of cloned cDNAs. *Nucleic Acids Res.* **12**, 7057–7070
46. Xia, Y., Chu, W., Qi, Q., and Xun, L. (2015) New insights into the QuikChangeTM process guide the use of Phusion DNA polymerase for site-directed mutagenesis. *Nucleic Acids Res.* **43**, e12
47. Waterhouse, A., Bertoni, M., Bienert, S., Studer, G., Tauriello, G., Gumienny, R., *et al.* (2018) SWISS-MODEL: homology modelling of protein structures and complexes. *Nucleic Acids Res.* **46**, W296–W303
48. Baconguis, I., Bohlen, C. J., Goehring, A., Julius, D., and Gouaux, E. (2014) X-ray structure of acid-sensing ion channel 1-snake toxin complex reveals open state of a Na(+)-selective channel. *Cell* **156**, 717–729

Mowgli Dandamudi is a Ph.D. student at the Sars International Centre for Marine Molecular Biology, University of Bergen, Norway. He studies the molecular basis of function in receptors from marine snails and worms, with a view to developing new pharmacological tools. While this study established useful pharmacological information, it uncovered surprising insight into the evolution of neuronal signaling in invertebrates.